

Dynamic identification of soil erosion risk in the middle reaches of the Yellow River Basin in China from 1978 to 2010

ZHAO Haigen^{1,2,3,4}, TANG Yuyu¹, YANG Shengtian^{1,2}

1. School of Geography, Beijing Normal University, Beijing 100875, China;

2. State Key Laboratory of Remote Sensing Science, Beijing Normal University, Beijing 100875, China;

3. Institute of Environment and Sustainable Development in Agriculture, Chinese Academy of Agricultural Sciences, Beijing 100081, China;

4. Beijing Water Science and Technology Institute, Beijing 100048, China

Abstract: Soil erosion has become a significant environmental problem that threatens ecosystems globally. The risks posed by soil erosion, the trends in the spatial distribution in soil erosion, and the status, intensity, and conservation priority level in the middle reaches of the Yellow River Basin were identified from 1978 to 2010. This study employed a multi-criteria evaluation method integrated with GIS and multi-source remote sensing data including land use, slope gradient and vegetation fractional coverage (VFC). The erosion status in the study region improved from 1978 to 2010; areas of extremely severe, more severe, and severe soil erosion decreased from 0.05%, 0.94%, and 11.25% in 1978 to 0.04%, 0.81%, and 10.28% in 1998, respectively, and to 0.03%, 0.59%, and 6.87% in 2010, respectively. Compared to the period from 1978 to 1998, the area classed as improvement grade erosion increased by about 47,210.18 km² from 1998 to 2010, while the area classed as deterioration grade erosion decreased by about 17,738.29 km². Almost all severe erosion regions fall in the 1st and 2nd conservation priority levels, which areas accounted for 3.86% and 1.11% of the study area in the two periods, respectively. This study identified regions where soil erosion control is required and the results provide a reference for policymakers to implement soil conservation measures in the future.

Keywords: dynamic identification; soil erosion risk; multi-criteria evaluation; multi-source remote sensing; Yellow River Basin

1 Introduction

Soil erosion is a well-known global environmental problem (Belyaev *et al.*, 2005; Deng *et al.*, 2009). It not only seriously threatens natural resources, infrastructure construction, and

Received: 2016-12-06 **Accepted:** 2017-03-21

Foundation: National Natural Science Foundation of China, No.41701517; National Key Project for R&D, No.2016YFC0402403, No.2016YFC0402409

Author: Zhao Haigen (1983–), PhD, specialized in hydrological simulation and remote sensing.

E-mail: zhaohaigen1983@163.com

***Corresponding author:** Yang Shengtian (1965–), Professor, E-mail: yangshengtian@bnu.edu.cn

agricultural production (Pimentel *et al.*, 1995; Lal, 1998; Park *et al.*, 2011; Sharda *et al.*, 2013), but also directly affects human safety and quality of life. Water erosion is one of the most serious types of soil erosion. Water erosion can result in land degradation by removing fertile topsoil layers, create negative downstream effects by depositing soil materials in rivers or reservoirs, and cause non-point pollution by washing pollutants attached to soil particles into natural waters (Vrieling *et al.*, 2008; Morgan, 2005; Wang *et al.*, 2013). Therefore, soil conservation is considered important for the protection of the environment and the economy.

China has suffered some of the most severe soil erosion on the planet. Between 2005 and 2007, almost 14% of the total soil erosion area in the world occurred in China (Li *et al.*, 2009). Water erosion constitutes the primary type of soil erosion in China and accounts for 45% of the total soil erosion area (Li *et al.*, 2008). Although the Chinese government has undertaken numerous soil conservation projects, the overall efficacy at improving environmental conditions is low (Zhang *et al.*, 2010). One reason for this low efficacy is that the allocation of limited human and financial resources for soil conservation is made based on the size of the watershed rather than the erosion conservation prioritization (Zhang *et al.*, 2002; Fan *et al.*, 2008). The identification of soil erosion risk can help map and monitor the spatial dynamics of erosion and conservation prioritization. Therefore, it is important to identify dynamic soil erosion risk to effectively use limited resources to control soil erosion in China.

Soil erosion is related to precipitation, land use, soil taxa, vegetation fractional coverage (VFC), and slope (Beskow *et al.*, 2009; Tian *et al.*, 2009). Water erosion is caused by rain and runoff, and its intensity can be expressed as the annual amount of surface soil loss (MWRC, 1997). Currently, both quantitative and qualitative methods are available for the identification of soil erosion. Among the quantitative methods, the experienced statistical universal soil loss equation (USLE) (Wischmeier and Smith, 1965), revised universal soil loss equation (RUSLE) (Renard *et al.*, 1991), and process-based physical water erosion prediction project model (WEPP) (Baffalt *et al.*, 1996) are widely used to simulate and estimate soil loss. Although quantitative methods can calculate absolute soil erosion amounts, their outcomes are generally applied qualitatively (Vrieling *et al.*, 2008). It is difficult to calculate soil erosion over long time periods or over large regions using quantitative methods because sufficient and accurate field validation measurements are time-consuming and expensive, and standard validation equipment is not easy to obtain (Stroosnijder, 2005; Vrieling *et al.*, 2008). In addition, the complexities in model structure, parameters, and scale effect also cause the calculated and measured results to differ (Boardman, 2006; Ni *et al.*, 2008). Compared to quantitative methods, qualitative approaches synthesize some important factors to show the relative probability of erosion. The identification of soil erosion risk using a qualitative method can usually meet the requirements, and accurate soil erosion determinations are often not necessary (Vrieling, 2006). With the help of a geographic information system (GIS), qualitative methods can also avoid the influence of personal subjective knowledge and can quickly and efficiently describe trends in soil erosion risk (Zhao *et al.*, 2002; Zhou and Wu, 2005; Masoudi and Patwardhan, 2006; Tian *et al.*, 2009; Zhang *et al.*, 2012; Zhu, 2012; Wang *et al.*, 2013).

Remote sensing at a regular spatial-temporal scale can provide detailed surface information and contribute to the assessment of regional and national erosion (Tian *et al.*, 2009; Siakeu

and Oguchi, 2000; Chen *et al.*, 2011; Aia *et al.*, 2013; Drzewiecki *et al.*, 2014; Aiello *et al.*, 2015). Previous research has established the multi-criteria evaluation (MCE) method integrated with GIS and remote sensing as a widespread qualitative method in the field; slope gradient, VFC, and land use are usually considered to be the key factors to assess soil erosion risk and identify priority areas for conservation (Eastman, 2001; Zhou *et al.*, 2005; Boroushaki and Malczewski, 2008; MWRC, 2008; Tian *et al.*, 2009; Beskow *et al.*, 2009; Chen *et al.*, 2011; Zhang *et al.*, 2012). Valente and Vettorazzi (2008) developed the spatial distribution of priority ranking in order to conserve forest resources in a river basin in Brazil. Zhang *et al.* (2010) identified the priority areas for controlling soil erosion in the Cetian reservoir area in China. Wang *et al.* (2013) assessed dynamic erosion risk in the Danjiangkou reservoir area in China using GIS and remote sensing data.

The middle reaches of the Yellow River are located on the Loess Plateau, a region with the most serious soil erosion caused by water in the world (Liu and Liu, 2010; Sun *et al.*, 2014). The Chinese government has undertaken numerous soil conservation projects in this region (Gao *et al.*, 2011). However, little research related to the identification of soil erosion risk has been conducted on large scales using multi-source remote sensing data with high spatial resolution. This research is particularly important because the Grain-for-Green Program, which began in 1998 (Fu *et al.*, 2011), has greatly improved the ecological and environmental quality in this region and is expected to have had an effect on soil erosion risk.

This study thus aims to use an efficient and fast MCE method that includes only three important factors to (1) analyze the dynamic trend in the spatial distribution of erosion status and intensity, and (2) identify the dynamic erosion risk in the middle reaches of the Yellow River Basin from 1978 to 2010. The results provide a scientific reference to help policy makers identify erosion control regions, create soil conservation measures, and implement new projects.

2 Study area

The study area (Figure 1) belongs to the middle reaches of the Yellow River Basin in China. It is located between 103°57'01"E–112°39'50"E and 33°40'19"N–40°35'43"N and covers the region between Hekouzhen and Tongguan hydrological stations. The total area is about $25 \times 10^4 \text{ km}^2$. The average annual precipitation is 300 mm in the northwest and 650 mm in the southeast, and most precipitation occurs as heavy rainstorms during the rainy season (Luo *et al.*, 2013). The major soil types distributed from the southeast to the northwest in this region include clayey loess, typical loess, sandy loess, and eolian sand (Liu, 1964). Corresponding to the soil distribution, the major vegetation type changes from broad-leaf deciduous forest to steppe and then to arid desert (Yang and Yuan, 1991). Wheat, corn, and millet are the major crops in this region.

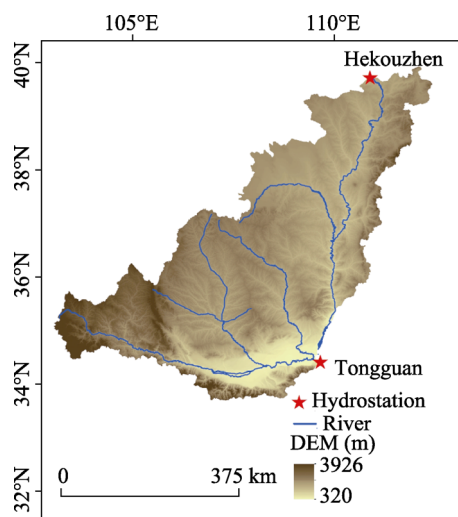


Figure 1 Location of the study area

3 Datasets

A digital elevation model (DEM) with a resolution of 90 m was used to generate the slope gradient. The DEM data were downloaded from the International Scientific and Technical Data Mirror Site, Computer Network Information Center, Chinese Academy of Sciences (<http://datamirror.csdb.cn>).

The multi-source remote sensing images used to interpret the land-use map and invert the VFC information included HJ-CCD, Landsat-TM, Landsat-MSS, and others. Table 1 gives details of the remote sensing data.

Table 1 Details of the remote sensing images in this study

Name	Resolution (m)	Acquired time	Acquired department
Landsat-MSS	56	July to September, 1978	NASA of the US
Landsat-TM	30	July to September, 1998	NASA of the US
HJ-CCD	32	July to September, 2010	China Center for Resources Satellite Data and Application
KH-11	3	July to September, 1978	NASA of the US
ZY3-CCD	2.1	July to September, 2012	China Center for Resources Satellite Data and Application
SPOT4	10	July to September, 1998	Yellow River Conservancy Commission in China

4 Methodology

4.1 MCE technique

The MCE technique is an evaluation decision-making method based on a series of criteria (Ceballos-Silva and López-Blanco, 2003). The main purpose of MCE is to investigate the complex tradeoffs between alternative choices with different environmental and socio-economic impacts (Krois, 2014). MCE could be used to conduct a quantitative treatment for the less quantifiable criteria and could synthetically consider the impact of multi-criteria on the object when making an objective evaluation. With the incorporation of GIS, MCE provides the optimal scheme for this purpose, using the weight linear combination and Boolean overlay. The integration of MCE within a GIS context could help users improve decision-making processes when solving conflictive situations for individuals or groups interested in spatial context (Malczewski, 1996; Ceballos-Silva, 2013).

4.2 Flowchart of methodology

The slope gradient, VFC, and soil taxa, which are related to land cover, can be used to indicate erosion resistance or risk; thus, land use, VFC, and slope gradient were used to assess the risk of soil erosion in this study (Zhang *et al.*, 2010).

Figure 2 shows a flowchart of the overall methodology used in this study based on the National Professional Standard SL190-2007 (MWRC, 2008), which was used to classify the grade of erosion risk. The slope gradient was calculated from DEM data with the help of ArcGIS software. The data for land use and VFC were mapped using remotely sensed images, as described in Section 3.

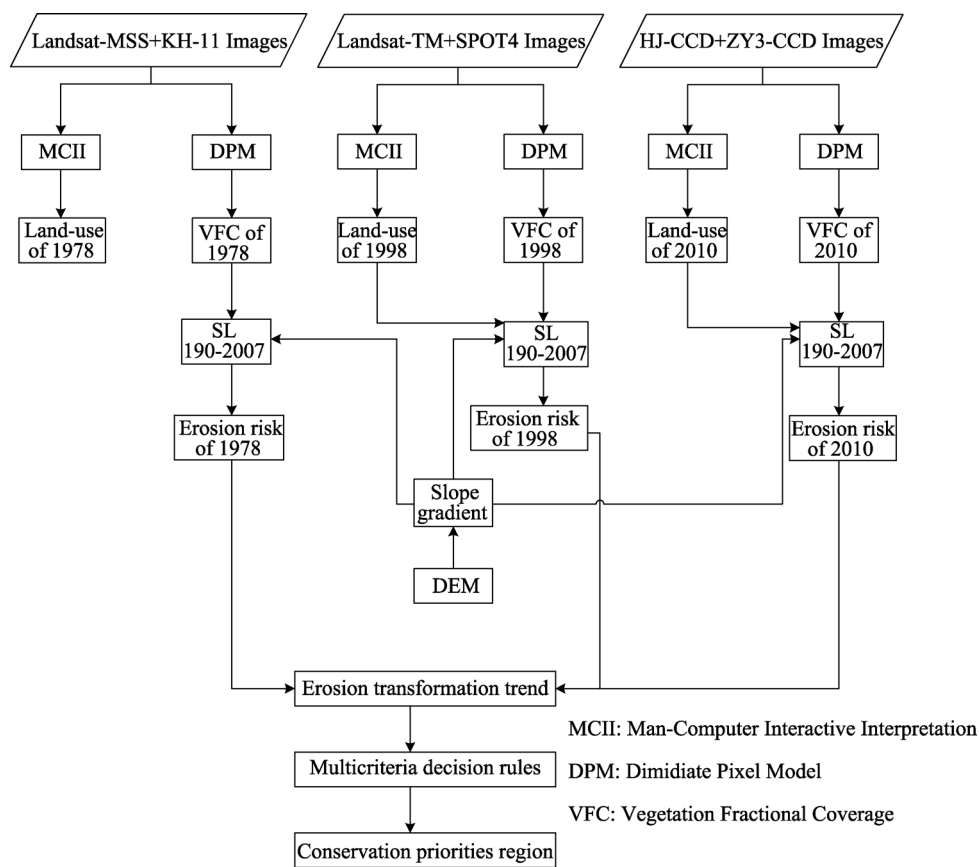


Figure 2 Flowchart of general methodology

In this study, soil erosion risk was classified into six grades: slight, light, moderate, severe, more severe, and extremely severe (Table 2) based on SL190-2007.

Table 2 Standards for the classification and gradation of soil erosion risk

Ground cover	VFC (%)	Slope (°)					
		< 5	5–8	8–15	15–25	25–35	> 35
Non-farmland	>75	Slight	Slight	Slight	Slight	Slight	Slight
	60–75	Slight	Light	Light	Light	Moderate	Moderate
	45–60	Slight	Light	Light	Moderate	Moderate	Severe
	30–45	Slight	Light	Moderate	Moderate	Severe	More severe
	<30	Slight	Moderate	Moderate	Severe	More severe	Extremely severe
Farmland		Slight	Light	Moderate	Severe	More severe	Extremely severe

4.3 Land use

In this study, the man-machine interactive visual interpretation method was first used to classify land-use types as forest, open woodland, other woodland, shrub, high-cover grassland, medium-cover grassland, low-cover grassland, farmland, water body, built-up land, or unused land, based on the land-use type classification standard of China. Subsequently, areas classified as forest, open woodland, other woodland, and shrub were further reclassified as forest-

land, and areas classified as high-, medium-, and low-cover grasslands were reclassified as grassland. Figure 3 shows the changes in land-use type over 33 years in the middle reaches of the Yellow River Basin.

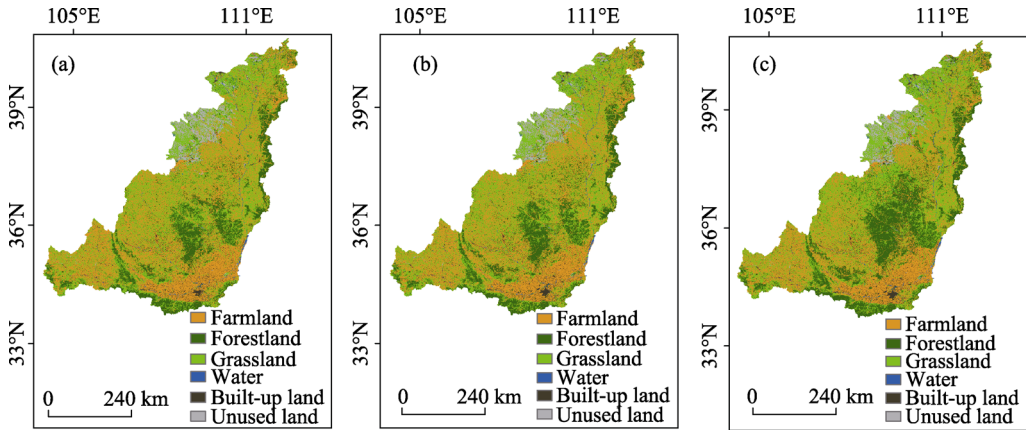


Figure 3 Land-use maps in the study area in 1978 (a), 1998 (b), and 2010 (c)

To assess the accuracy of the interpretation of land use, 129 field verification points covering approximately 32% of the study area were collected using GPS. In 2010, 129 samples were validated; the results showed that 121 were correctly identified, giving an interpretation accuracy of 93.8%. For land use in 1998, multiple types of information, including historical documents, maps, and interviews with local residents, were employed to determine the interpretation accuracy. In addition, for land use in 1978, the KH-11 data were used to validate the interpretation accuracy. The results showed that the overall accuracy in both 1998 and 1978 was approximately 85%.

4.4 VFC

Vegetative growth and cover can be reflected by the normalized difference vegetation index (NDVI). The NDVI can eliminate remote sensing irradiation errors to some extent. To retrieve the VFC, the following functions based on NDVI were used in this study:

$$VFC = (NDVI - NDVI_{soil}) / (NDVI_{veg} - NDVI_{soil}) \quad (1)$$

where VFC is vegetation fractional coverage, $NDVI_{soil}$ is the $NDVI$ of barren soil, and $NDVI_{veg}$ is the $NDVI$ of vegetation;

$$NDVI = (NIR - R) / (NIR + R) \quad (2)$$

where NIR is the reflectivity of the near-infrared band, and R is the reflectivity of the red band.

To fully cover the relatively large study area, images for different days were collected and used to address the influence of cloud cover and satellite orbit. To minimize the errors caused by the imaging times of adjacent $NDVI$ images, an adjacent image regression analysis, as described in Zhou *et al.* (2015), was adopted. The accuracy of the resulting VFC for the three periods was assessed using the methodology of Zhou *et al.* (2015) and the result indicated that the overall accuracy was more than 86%. In addition, the accuracy of data obtained for land use and VFC was also identified and accepted at a meeting held by experts from the Yellow

River Conservancy Commission of the Ministry of Water Resources at Zhengzhou city in China.

Based on SL190-2007, the VFC was reclassified into five classes, with limits of 30%, 45%, 60%, and 75%. Figure 4 shows the changes of VFC from 1978 to 2010.

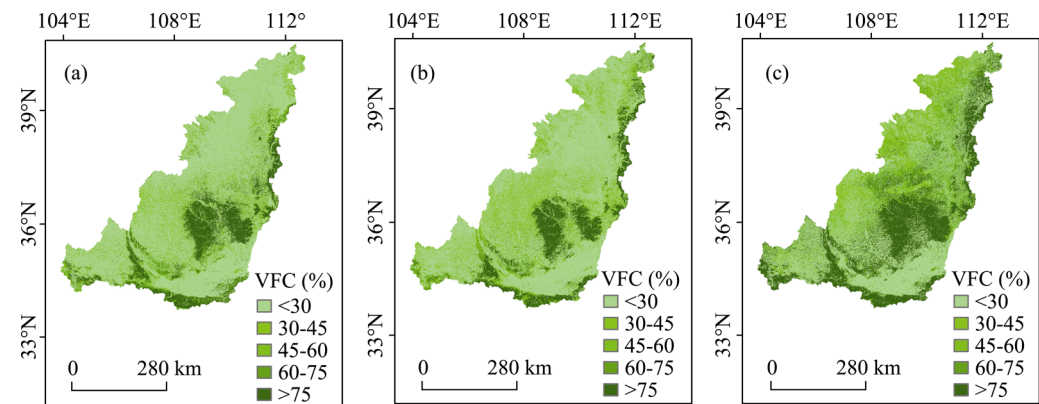


Figure 4 Vegetation fractional coverage (VFC) maps in the study area in 1978 (a), 1998 (b) and 2010 (c)

4.5 Slope gradient

Slope gradient is an important reflection of surface undulation and can change the hydrological velocity and the direction of surface runoff. Thus, slope gradient has a significant impact on surface hydrological processes and soil erosion (Beskow *et al.*, 2009). In this study, DEM data in the range of 320 to 3296 m were used to generate the slope gradient with ArcGIS software and the algorithm described by Burrough in 1998. In this study, the slope gradient was reclassified with threshold values of 5°, 8°, 15°, 25° and 35° based on SL190-2007 (Figure 5).

5 Results

5.1 Identification of soil erosion risk

The six classes of slope gradient (Table 2) in the middle reaches of the Yellow River Basin account for 29.01%, 12.53 %, 31.57%, 22.87%, 3.47%, and 0.55% of the total study area, respectively.

The proportions of the different classes of VFC and different land-use types in 1978, 1998, and 2010 are listed in Tables 3 and 4. Table 3 shows that from 1978 to 1998 the low-cover classes of vegetation (<30% and 30%–45%) increased by 1.83%, the medium-cover classes (45%–60%) did not significantly change, and the high-cover classes (60%–75% and > 75%) decreased by 2.21%. From 1998 to 2010, the low-cover classes of vegetation decreased by

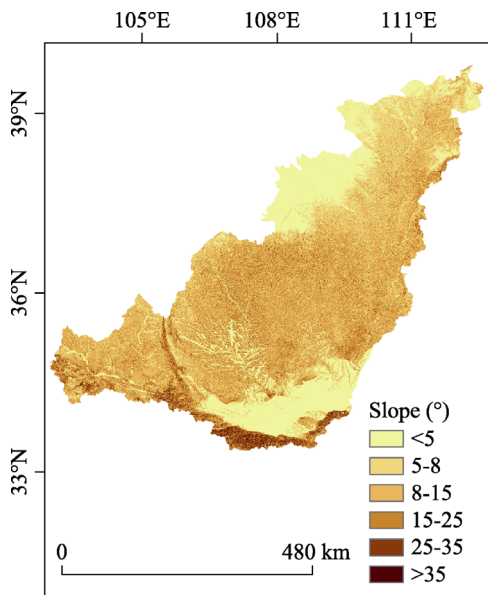


Figure 5 Ranks of slope gradient in the study area

25.22%, the medium-cover classes increased by 4.67%, and the high-cover classes increased by 20.55%. Compared to the changes in VFC between 1978 and 1998, there was a significant reduction in the low-cover classes of vegetation and an increase in the high-cover classes of vegetation from 1998 to 2010.

The change in land use described in Table 4 is consistent with the changes in VFC detailed above. The change in land use was not significant from 1978 to 1998. However, between 1998 and 2010, forest and grassland areas increased, and farmland area decreased. The proportion of farmland decreased by 3.90% of the total study area, and the proportion of farmland and forest land increased by 4.07% of the total study area.

The distributions of soil erosion risk grades in the study area in 1978, 1998, and 2010 were identified using the standards in Table 2. Figure 6 shows the spatial dynamics of erosion risk grades from 1978 to 2010. No significant changes were observed between 1978 and 1998, and the overall erosion status improved between 1998 and 2010, particularly in the high-sediment region. One reason for this phenomenon is the large-scale implementation of the Grain-for-Green Program in the study area.

Table 3 Proportions of different classes of VFC in the study area from 1978 to 2010 (%)

Proportion (%)	1978	1998	2010
<30	62.23	57.28	39.94
30–45	10.30	17.08	9.20
45–60	7.45	7.83	12.50
60–75	6.16	5.43	12.01
>75	13.86	12.38	26.35

Table 4 Proportions of different land-use types in the study area from 1980 to 2010 (%)

Land use type	1980	1998	2010
Farmland	38.57	37.42	33.52
Forestland	15.85	16.70	21.65
Grassland	39.22	39.49	38.61
Water	0.93	0.93	0.59
Built-up land	2.01	2.22	2.34
Unused land	3.42	3.24	3.29

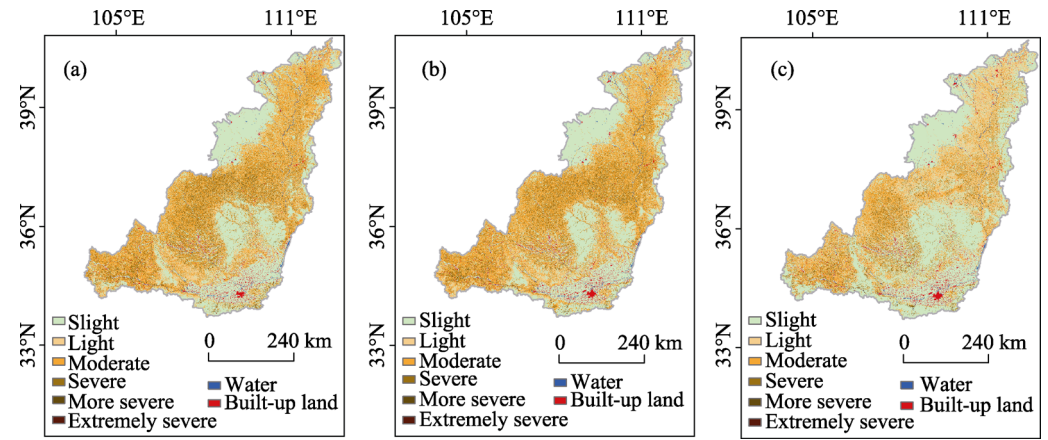


Figure 6 Soil erosion risk grades in the study area in 1978 (a), 1998 (b), and 2010 (c)

The accuracy of the identified erosion risk in 2010 was assessed based on randomly selected field samples and judged primarily by the knowledge of experts from the Yellow River Conservancy Commission of the Ministry of Water Resources. The results indicate that the overall accuracy of estimated erosion risk was 90.5% in 2010. This accuracy level confirms

that the accuracy identified for 1978 and 1998 can also be used because the erosion risk maps for all three periods were generated based on slope, VFC, and land use data, and the accuracies of VFC and land use were satisfactory, as described in the validation result in Section 3.

5.2 Comparison of soil erosion risk

Table 5 shows obvious changes in the proportions of erosion risk grades from 1978 to 1998 and from 1998 to 2010, although the trends in the proportions of the severe, more severe, and extremely severe grades were similar in the two periods.

Table 5 Distributions of soil erosion risk grades in the study area in 1978, 1998, and 2010

Erosion risk grade	Erosion risk in 1978		Erosion risk in 1998		Erosion risk in 2010	
	Area (km ²)	Proportion (%)	Area (km ²)	Proportion (%)	Area (km ²)	Proportion (%)
Slight	105516.21	42.22	103337.17	41.35	132991.81	53.21
Light	34582.84	13.84	36547.61	14.62	56912.95	22.77
Moderate	79221.49	31.70	82230.37	32.90	41308.32	16.53
Severe	28114.40	11.25	25683.34	10.28	17157.76	6.87
More severe	2356.23	0.94	2033.02	0.81	1472.78	0.59
Extremely severe	129.89	0.05	89.55	0.04	77.42	0.03

The area with a soil erosion risk grade of severe decreased from 28,114.40 km² (11.25% of the region's total area) in 1978 to 25,683.34 km² (10.28%) in 1998, and to 17,157.76 km² (6.87%) in 2010. The area graded more severe decreased from 2356.23 km² (0.94%) in 1978 to 2033.02 km² (0.81%) in 1998, and 1472.78 km² (0.59%) in 2010. The area with a grade of extremely severe decreased from 129.89 km² (0.05%) in 1978 to 89.55 km² (0.04%) in 1998, and 77.42 km² (0.03%) in 2010. In contrast, the total area with grades of slight, light, and moderate soil erosion risk increased from 219,320.54 km² (87.76%) in 1978 to 222,115.15 km² (88.87%) in 1998, and 231,213.08 km² (82.51%) in 2010. The results shown in Table 2 illustrate that from 1978 to 2010 the overall erosion status improved in the study area.

In order to further understand the transformations in erosion grades occurring in the different time periods, the transformation between successive periods, demonstrated by overlaying the erosion risk results in two adjacent periods pixel by pixel, is expressed as a proportion for each erosion grade (Tables 6 and 7).

Table 6 Proportion of transformation for each erosion grade in the study area between 1978 and 1998

		Erosion grade in 1998 (%)					
		Slight	Light	Moderate	Severe	More severe	Extremely severe
Erosion grade in 1978 (%)	Slight	35.30	2.06	1.72	0.20	0.02	0.002
	Light	1.70	8.85	3.14	0.14	0	0
	Moderate	1.20	3.58	25.91	0.96	0.05	0.001
	Severe	0.16	0.13	2.07	8.84	0.05	0.001
	More severe	0.04	0	0.07	0.14	0.70	0.002
	Extremely severe	0.01	0	0.004	0.003	0.002	0.03

Table 6 shows the transformation matrix of the proportional distribution of each erosion grade between 1978 and 1998. The values located diagonally from the upper-left corner to the

lower-right corner represent the proportions of unchanged areas in the study area. The values above the diagonal represent the proportions of areas with increased erosion risk, while the values below the diagonal represent the proportions with reduced risk. From 1978 to 1998 (Table 6), the unchanged proportion accounts for 79.63% of the region’s total area, with the unchanged proportions of areas of slight, light, moderate, severe, more severe, and extremely severe erosion risk accounting for 44.33%, 11.11%, 32.54%, 11.10%, 0.88%, and 0.04% of the total unchanged area, respectively. The high proportion of unchanged area illustrates that erosion risk did not change significantly between 1978 and 1998. The grades of slight, light, and moderate risk account for the majority of the changed area, and changes from moderate to slight and moderate to light represent the largest proportion (4.78%) of reduced erosion risk from 1978 to 1998. In contrast, the changes from slight and light to moderate represent the largest proportion (4.86%) of increased erosion risk in this period. These results illustrate that the overall erosion status was stable from 1978 to 1998, and areas of improvement and deterioration coexisted.

Table 7 Proportion of transformation for each erosion grade in the study area between 1998 and 2010

		Erosion grade in 2010 (%)					
		Slight	Light	Moderate	Severe	More severe	Extremely severe
Erosion grade in 1998 (%)	Slight	38.06	0.35	0.13	0.07	0.02	0.004
	Light	4.66	8.78	0.29	0.05	0	0
	Moderate	5.86	12.74	14.38	0.25	0.03	0.003
	Severe	0.97	1.15	1.72	6.51	0.02	0.001
	More severe	0.08	0	0.17	0.05	0.52	0.001
	Extremely severe	0.010	0	0.001	0.002	0.001	0.02

Table 7 shows that from 1998 to 2010, the unchanged proportion was 68.27% of the total study area, with the unchanged proportions of slight, light, moderate, severe, more severe, and extremely severe risk accounting for 51.71%, 12.86%, 21.06%, 9.54%, 1.03%, and 0.004% of the total unchanged area, respectively. These results indicate clear changes in erosion grade between 1998 and 2010. In this period, the greatest reductions in erosion risk were from moderate to slight and light, severe to slight and light, and light to slight, which accounted for 18.60%, 2.12%, and 1.70% of the study area, respectively. The areas with increased erosion risk were very small, the largest value being 0.29%.

5.3 Trend analysis of erosion transformation

Based on Figure 6, the erosion trends between 1978 and 1998 and between 1998 and 2010 were mapped (Figure 7), and the statistical results for the two periods are shown in Table 8.

Figure 7 shows the spatial distributions of changes in erosion grade from 1978 to 1998 and from 1998 to 2010. From 1978 to 1998, some erosion grades improved, while others deteriorated (Figure 7a), but from 1998 to 2010, there were 20 times more improvements in grade than deteriorations (Figure 7b).

Table 8 shows that most deteriorations and improvements in the grade of soil erosion risk were changes of one or two grades. The total area where the erosion grade improved from 1998 to 2010 (28.18% of the region’s total area) was obviously greater than that from 1978 to

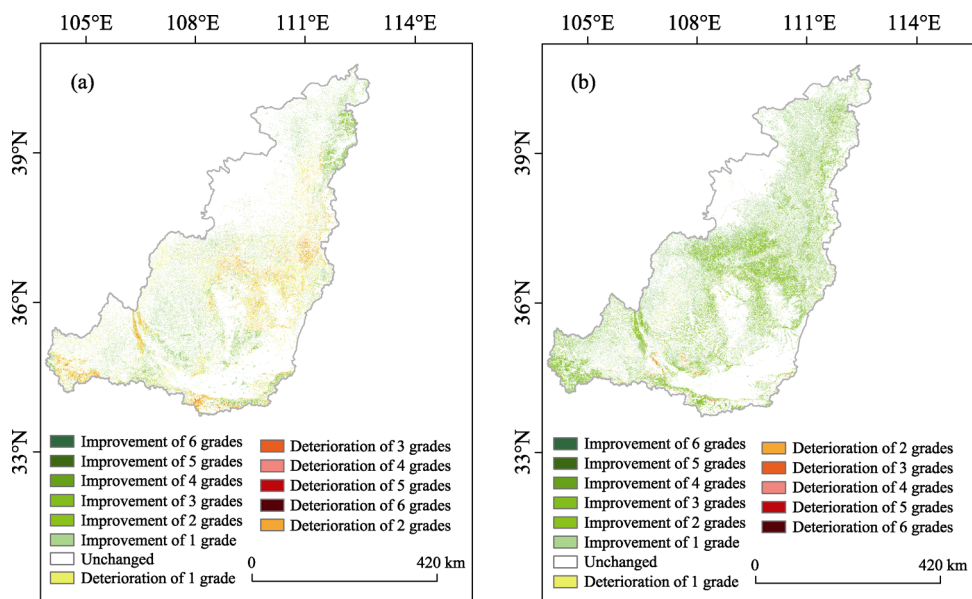


Figure 7 Changes in erosion risk grades in the study area from 1978 to 1998 (a) and from 1998 to 2010 (b)

Table 8 Deterioration and improvement in erosion grades in the study area between 1980 and 2010

Erosion grade variation	1978 to 1998		1998 to 2010	
	Area (km ²)	Proportion (%)	Area (km ²)	Proportion (%)
Deterioration of 1 grade	15508.13	6.21	2303.26	0.92
Deterioration of 2 grades	4780.16	1.91	534.25	0.21
Deterioration of 3 grades	491.20	0.20	193.21	0.08
Deterioration of 4 grades	51.78	0.02	56.92	0.02
Deterioration of 5 grades	4.50	0.002	9.83	0.004
Improvement of 1 grade	19141.65	7.66	50004.85	20.01
Improvement of 2 grades	3481.08	1.39	17731.47	7.09
Improvement of 3 grades	445.28	0.18	2463.94	0.99
Improvement of 4 grades	116.81	0.05	206.87	0.08
Improvement of 5 grades	36.21	0.01	24.08	0.01
Summation of deterioration grades	20835.77	8.34	3097.48	1.23
Summation of improvement grades	23221.03	9.29	70431.21	28.18

1998 (9.29%). The total area that saw a deterioration in erosion grade from 1998 to 2010 (1.23% of the region’s total area) was obviously less than that from 1978 to1998 (8.34%). These results indicate that the erosion condition has been improving in recent years. Although the area at high risk of erosion is decreasing, erosion risk should not be ignored in government policies related to soil conservation. The results shown in Figure 7 are consistent with those in Table 8 and indicate the spatial areas of soil erosion measures.

5.4 Identification of conservation priorities

The conservation priorities of regions were identified by analyzing changes in erosion risk.

Table 9 shows the conservation priorities created based on SL190-2007. A higher conservation priority corresponds to a greater erosion risk and indicates that more attention should be given to that region. Based on Table 9, the proportion and the area of every priority level are shown in Table 10.

Table 9 Multi-criteria decision rules for identifying conservation priorities

		Erosion grade in the next period					
		Slight	Light	Moderate	Severe	More severe	Extremely severe
Erosion grade in the previous period	Slight	IV	IV	II	I	I	I
	Light	IV	IV	III	II	I	I
	Moderate	IV	V	III	II	II	I
	Severe	IV	V	IV	III	II	I
	More severe	IV	V	IV	III	II	I
	Extremely severe	IV	VI	V	IV	III	I

Table 10 Area and proportion of each priority level in the study area

Priority level	1978 to 1998		1998 to 2010	
	Area (km ²)	Proportion (%)	Area (km ²)	Proportion (%)
1st level	627.06	0.25	298.80	0.12
2nd level	9023.28	3.61	2464.15	0.99
3rd level	95046.16	38.03	52536.04	21.02
4th level	32618.80	13.05	27296.90	10.92
5th level	9280.42	3.71	34332.97	13.74
6th level	103325.32	41.34	132992.19	53.21

Table 10 indicates that areas with severe erosion and at the 1st and 2nd priority levels comprised 9650.34 km² (3.86% of the region’s total area) from 1978 to 1998 and 2762.95 km² (1.11%) from 1998 to 2010. Although the area at severe risk of erosion is becoming smaller, it should not be ignored and requires constant attention to ensure appropriate erosion measures in future projects. The 3rd and 4th levels accounted for 51.08% and 31.94% of the region’s total area from 1978 to 1998 and from 1998 to 2012, respectively. These two levels represent stable or slightly changing erosion status and indicate the need for only a minor allocation of resources to control soil erosion. The areas represented by the 5th and 6th levels accounted for 45.05% and 66.95% of the study area from 1978 to 1998 and from 1998 to 2012, respectively. These areas have low erosion risk, and the current development intensity should be maintained without the need for extra measures to control soil erosion. Compared to the period from 1978 to 1998, the control of soil erosion has been remarkably successful from 1998 to 2010.

Based on the results shown in Tables 9 and 10, distribution maps of conservation priority levels from 1978 to 2010 were generated (Figure 8). Figure 8 can provide comparative measures for controlling soil erosion from 1978 to 2010 for government, and thus facilitates the efficient use of labor and funds to control soil erosion in the future.

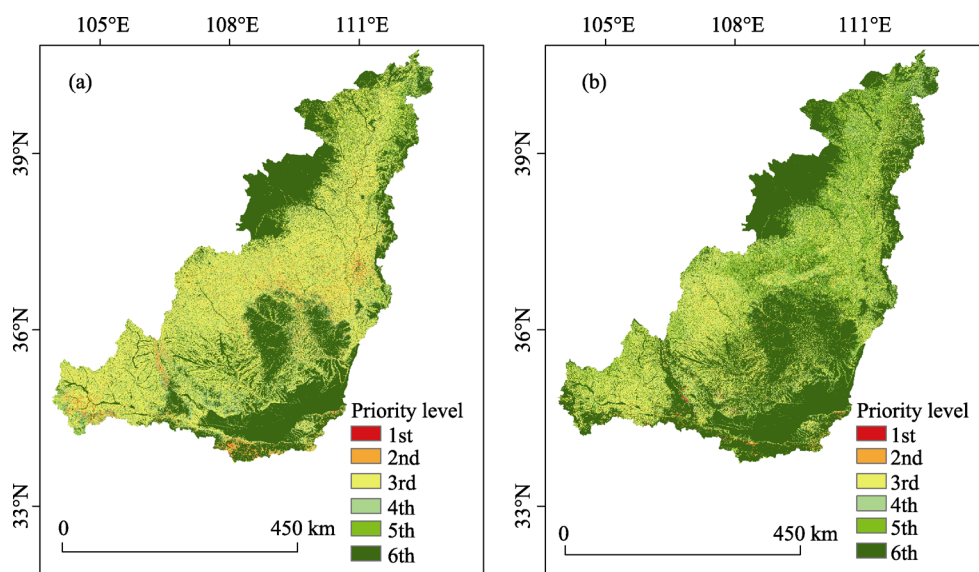


Figure 8 Maps showing the distributions of conservation priority levels in the study area from 1978 to 1998 (a) and from 1998 to 2010 (b)

6 Discussion

Water erosion is known to be the most important factor causing soil degradation worldwide. The middle reaches of the Yellow River Basin on the Loess Plateau are one of the regions most seriously affected by water erosion in the world. Therefore, this area is an important conservation region for the control of soil erosion. Sedimentation rates and human activity are significantly correlated. From the end of the 1970s to the end of the 1990s, a series of soil and water conservation projects were carried out under the support of government-sponsored programs in the area. At the same time, a strong economy led to increased deforestation in this period; thus, improvements in erosion were accompanied by some deteriorations. After 1999, the implementation of the large-scale Grain-for-Green Program greatly increased the proportions of forest and grasslands in the study area and reduced the overall intensity of soil erosion. Therefore, analyzing the temporal and spatial distribution dynamics of soil erosion risk and identifying priority regions over the past 33 years is important for government policymaking in the future.

6.1 Selection of criteria for the dynamic identification of soil erosion risk

The average slope gradient can change with variation in the spatial resolution of DEM data (David and McCabe, 2000; Thompson *et al.*, 2001; Wang and Wang, 2009; Fu, 2015). Previous studies (Sun *et al.*, 2013; Sun *et al.*, 2014) have shown that DEM data with a resolution of 90 m can be used to calculate the erosion rate at a large scale in the Loess Plateau region. Thus, in order to balance the time cost and accuracy of calculation, a resolution of 90 m was chosen in this study. However, the spatial effects of the DEM resolution on the generation of erosion risk in such a large region should be identified in future research.

Land-use factors were separated into farmland and non-farmland types to calculate the spatial and temporal changes in erosion risk from 1978 to 2010. However, in reality, the soil conservation functions of forestland and grassland are different, even if they have the same

VFC. Generally, forest has deeper root length, a larger root distribution area, and a denser canopy than grassland. Thus, forest can more greatly reduce the percussive force of a raindrop, can intercept more rainfall, and is better at controlling soil erosion. Quantitative differences in land-use types should be considered when calculating soil erosion risk in future research.

Three periods of remote sensing data were employed to generate land use, slope gradient, and VFC, which have key effects on the distribution of erosion risk. The remote sensing data used to generate these land-use and VFC data included Landsat TM, Landsat MSS, and HJ-CCD. Although the sensors of Landsat and HJ are different, Landsat and HJ have similar spectral ranges in the first four bands, and the difference in spatial resolution between MSS and TM is acceptable. In addition, the remote sensing data were obtained between July and August, because these data best reflect the growth status of vegetation. Therefore, it is reasonable to compare the risk maps for the three time periods.

When assessing soil erosion, the MCE used in this study does not consider rainfall intensity, unlike the RUSLE model (Lu *et al.*, 2004; Alexakis *et al.*, 2013; Fu *et al.*, 2013). Although the RUSLE function reflects erosion more physically (for example, by considering the impacts of climate and underground and raindrop kinetic energy), it requires more accurate input data and is likely to produce significant errors in a specific rainfall measurement if the region has complex terrain and diverse physiognomy (Wang *et al.*, 2013). The distribution of national meteorological stations that can provide publicly available data in the study area is uneven and scarce; thus, it is difficult to use the geographic interpolation method to obtain high-resolution and continuous raster data that can accurately describe the spatial variations in precipitation (Meusburger *et al.*, 2012). Nevertheless, rainfall intensity and runoff should be considered in future risk assessment models.

6.2 Comparison between soil erosion risk grades and estimated soil loss

To further identify the accuracy of soil erosion risk grades, the distribution of soil risk grades in this study were compared with the results of Fu *et al.* (2011). Figure 9 shows the distributions of estimated soil loss calculated by the USLE method. The spatial patterns of soil erosion risk grades in Figure 6 are generally consistent with the distributions of estimated soil losses shown in Figure 9. The regions classified as having slight, light, moderate, severe, more severe, and extremely severe erosion risk in Figure 6 basically correspond to the soil

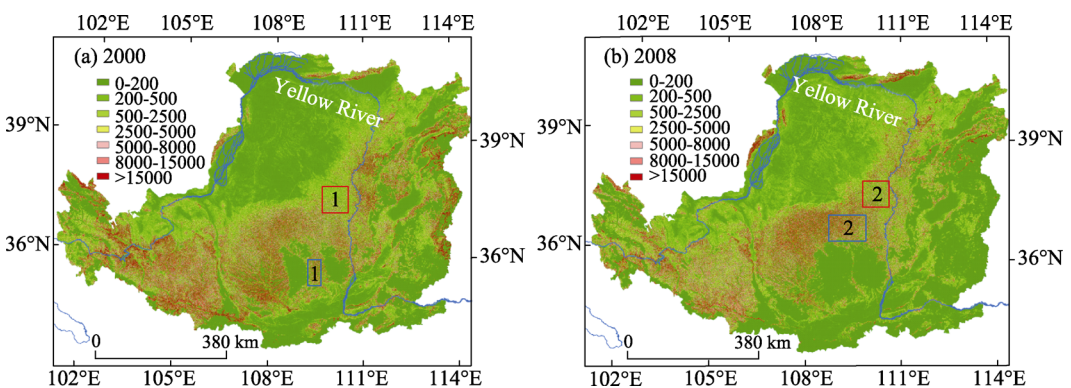


Figure 9 Spatial distributions of estimated soil loss ($t\ km^{-2}\ yr^{-1}$) in the study area in 2000 (a) and 2008 (b) (Fu *et al.*, 2011)

loss ranges of 0–500, 500–2500, 2500–5000, 5000–8000, 8000–15000, and >15000, respectively, in Figure 9. However, there are differences between them in some areas.

Some areas have moderate erosion risk (blue box 1) or slight erosion risk (blue box 2) in Figure 9, but fall in the soil loss range of >8000 in Figure 9. These areas are forestlands, and these discrepancies may be primarily attributed to differences in the vegetation cover data. In this study, the VFC values in 1998 and 2010 were derived respectively from Landsat-TM with a resolution of 30 m and HJ-CCD with a resolution of 32 m. In Figure 9, the maximum 16-day NDVI data were derived from MODIS images with a resolution of 250 m. This higher-resolution VFC data should alleviate the soil erosion risk grade.

Some areas have severe and more severe risk grades in Figure 6, but fall into the soil loss range of 500–2500 in Figure 9 (red box 1). Some areas have moderate or severe risk grades in Figure 6, but fall into the soil loss range of 0–500 in Figure 9 (red box 2). These areas are farmlands, and these discrepancies are caused by the differences in the methods used to treat vegetation and slope. In this study, VFC was not considered, and the absolute slope gradient was used when calculating the soil erosion grades for farmland. In Figure 9, vegetation was considered, and the percentile slope gradient was used when calculating soil erosion. Thus, compared to the results of this study, the soil erosion grades in the literature are lower.

In addition, the time periods considered in this study are different from those in the literature, which could obviously affect the vegetation data and the results of the comparisons among different time periods. Thus, more field data should be collected to validate the study results.

However, the maps showing the distributions of conservation priority levels in this study (Figure 8) demonstrated that the change of soil erosion control as an ecosystem service driven by the vegetation cover change mainly happened on the slopes. In this regard, the results of this study are meaningful to assess the dynamics of soil erosion risk, and thus the evolution of the soil erosion control service on the Loess Plateau.

7 Conclusions

Based on GIS techniques, this study integrated a multi-criteria evaluation approach involving high-spatial-resolution remote sensing data (slope gradient, VFC, and land use) to qualitatively identify the trends in the spatial distribution of soil erosion risk in the middle reaches of the Yellow River Basin from 1978 to 2010.

The results show that erosion risk has decreased over the 33-year study period. From 1978 to 1998, the areas categorized as having extremely severe, more severe, and severe erosion risk decreased by 0.01%, 0.13%, and 0.97% of the study area, respectively; the respective decreases were 0.01%, 0.22%, and 3.41%. The decreasing trend from 1998 to 2010 was more pronounced than that from 1978 to 1998.

The results also indicate that from 1978 to 2010 the total area classed as deterioration grade erosion was smaller than that classed as improvement grade erosion, and that the transformation between these classes between 1998 and 2010 was smaller than that between 1978 and 1998. From 1978 to 1998, the proportions of the region where the erosion grade changed from severe to slight and from severe to light were 0.16% and 0.13%, respectively, and the proportions of regions where the erosion grade changed from slight and light to extremely severe

and severe were all less than 0.01%. From 1998 to 2010, the proportions of regions where the erosion grade changed from severe to slight and from severe to light were 0.97% and 1.15%, respectively, and the proportions of regions where the erosion grade changed from slight or light to extremely severe or severe were all less than 0.01%. The proportions of extremely severe and more severe erosion grades were all less than 0.01% of the total area from 1978 to 1998 and from 1998 to 2010, but these values were greater from 1998 to 2010 than from 1978 to 1998.

Compared to the period from 1978 to 1998, the area of improvement grade erosion increased by about 47210.18 km² from 1998 to 2010, while the area of deterioration grade erosion decreased by about 17738.29 km². The changes in erosion risk indicated that the regions in which erosion risk increased or decreased significantly were located in the central region of the study area.

The maps of the distributions of conservation priority levels indicate that conservation priority levels are significant for future eco-environment management and policymaking related to water and soil conservation in the Yellow River Basin. The top two conservation priorities accounted for 3.86% and 1.11% of the total study area. These areas should not be ignored; they should be given attention even though their overall erosion intensity has been reduced.

The MCE model integrated with multi-source remote sensing data can be applied in the middle reaches of the Yellow River Basin. The dynamics of the spatial distribution of erosion risk from 1978 to 2010 can provide guidance for government agencies as they plan water conservation efforts and implement soil conservation projects in the future.

References

- Aia L, Fang N F, Zhang B *et al.*, 2013. Broad area mapping of monthly soil erosion risk using fuzzy decision tree approach: Integration of multi-source data within GIS. *International Journal of Geographical Information Science*, 27: 1251–1267.
- Aiello A, Adamo M, Canora F, 2015. Remote sensing and GIS to assess soil erosion with RUSLE3D and USPED at river basin scale in southern Italy. *Catena*, 131: 174–185.
- Alexakis D D, Hadjimitsis D G, Agapiou A, 2013. Integrated use of remote sensing, GIS and precipitation data for the assessment of soil erosion rate in the catchment area of “Yialias” in Cyprus. *Atmospheric Research*, 131: 108–112. doi: 10.1016/j.atmosres.2013.02.013.
- Baffalt C, Nearing M A, Nicks A D, 1996. Impact of GLIGEN parameters on WEPP predicted average soil loss. *Transactions of the ASAE*, 2: 1001–1020.
- Belyaev V, Wallbrink P, Golosov V N *et al.*, 2005. A comparison of methods for evaluating soil redistribution in the severely eroded Stavropol region, southern European Russia. *Geomorphology*, 65: 173–193.
- Beskow S, Mello C R, Norton L D *et al.*, 2009. Soil erosion prediction in the Grande River Basin, Brazil using distributed modeling. *Catena*, 79: 49–59.
- Boardman J, 2006. Soil erosion science: Reflections on the limitations of current approaches. *Catena*, 68: 73–86.
- Borouhaki S, Malczewski J, 2008. Implementing an extension of the analytical hierarchy process using ordered weighted averaging operator with fuzzy quantifiers in ArcGIS. *Computers & Geosciences*, 34: 399–410.
- Carlson T N, Ripley D A, 1998. On the relation between NDVI, fractional vegetation coverage, and leaf area index. *Remote Sensing of Environment*, 62: 241–252.
- Ceballos-Silva A, López-Blanco J, 2003. Delineation of suitable areas for crops using a multi-criteria evaluation approach and land use/cover mapping: A case study in Central Mexico. *Agricultural Systems*, 77: 117–136.
- Chen T, Niu R Q, Li P X *et al.*, 2011. Regional soil erosion risk mapping using RUSLE, GIS, and remote sensing: A case study in Miyun Watershed, North China. *Environmental Earth Sciences*, 63: 533–541.

- David M W, McCabe G J, 2000. Differences in topographic characteristics computed from 100- and 1000-m resolution digital elevation model data. *Hydrological Processes*, 14: 987–1002.
- Deng Z Q, Lima J, Jung H S, 2009. Sediment transport rate-based model for rainfall induced soil erosion. *Catena*, 76: 54–62.
- Drzewiecki W, Wężyk P, Pierzchalski M *et al.*, 2014. Quantitative and qualitative assessment of soil erosion risk in Małopolska (Poland), supported by an object-based analysis of high-resolution satellite images. *Pure and Applied Geophysics*, 171: 867–895.
- Eastman J R, 2001. IDRISI 32: Guide to GIS and Image Processing. Worcester, USA: Clark Labs, Clark University.
- Fan H M, Wang T L, Cai Q G *et al.*, 2008. Study on the zonation differentiation of soil erosion and the model of soil and water conservation in northeast China. *Research of Soil and Water Conservation*, 15: 69–72. (in Chinese)
- Fu B J, Liu Y, Lü Y H *et al.*, 2011. Assessing the soil erosion control service of ecosystems change in the Loess Plateau of China. *Ecological Complexity*, 8: 284–293.
- Fu S H, Cao L X, Liu B Y *et al.*, 2015. Effects of DEM grid size on predicting soil loss from small watersheds in China. *Environmental Earth Sciences*, 73: 2141–2151.
- Gao P, Mu X M, Wang F *et al.*, 2011. Changes in streamflow and sediment discharge and the response to human activities in the middle reaches of the Yellow River. *Hydrology and Earth System Sciences*, 15: 1–10.
- Krois J, Schulte A, 2014. GIS-based multi-criteria evaluation to identify potential sites for soil and water conservation techniques in the Ronquillo watershed, northern Peru. *Applied Geography*, 51: 131–142.
- Lal R, 1998. Soil erosion impact on agronomic productivity and environment quality. *Critical Reviews in Plant Sciences*, 17: 319–464.
- Li R, Shangguan Z, Liu B *et al.*, 2009. Advances of soil erosion research during the past 60 years in China. *Journal of Soil and Water Conservation*, 5: 1–6. (in Chinese)
- Li Z, Cao W, Liu B *et al.*, 2008. Current status and developing trend of soil erosion in China. *Journal of Soil and Water Conservation*, 1: 57–62. (in Chinese)
- Lu D, Li G, Valladares G S *et al.*, 2004. Mapping soil erosion risk in Rondônia, Brazilian Amazonia: Using RUSLE, remote sensing and GIS. *Land Degradation & Development*, 15: 499–512.
- Liu D S, 1964. Loess in the Middle Yellow River Drainage Basin. Beijing, China: Science Press: (in Chinese)
- Liu L, Liu X H, 2010. Sensitivity analysis of soil erosion in the northern Loess Plateau. *Procedia Environmental Sciences*, 2: 134–148.
- Luo Y, Yang S T, Zhao C S *et al.*, 2013. The effect of environmental factors on spatial variability in land use change in the high-sediment region of China's Loess Plateau. *Journal of Geographical Sciences*, 24: 802–814.
- Malczewski J A, 1996. GIS-based approach to multiple criteria group decision-making. *International Journal of Geographical Information Science*, 10(8): 321–339.
- Masoudi M, Patwardhan A M, 2006. Risk assessment of water erosion for the Qareh Aghaj subbasin, southern Iran. *Stochastic Environmental Research and Risk Assessment*, 21: 15–24.
- Meusburger K, Steel A, Panagos P *et al.*, 2012. Spatial and temporal variability of rainfall erosivity factor for Switzerland. *Hydrology and Earth System Sciences*, 16: 167–177.
- Morgan R P C, 2005. Soil Erosion and Conservation, 3rd ed., Blackwell Publishing Company: Malden, MA, USA.
- MWRC (Ministry of Water Resources of China), 1997. National Professional Standards for Classification and Gradation of Soil Erosion, SL 190-1996. Beijing, China. (in Chinese)
- MWRC (Ministry of Water Resources of China), 2008. SL190–2007: Standards for Classification and Gradation of Soil Erosion. Beijing, China: Water Resources & Hydropower Press of China. (in Chinese)
- Ni G H, Liu Z Y, Lei Z D *et al.*, 2008. Continuous simulation of water and soil erosion in a small watershed of the Loess Plateau with a distributed model. *Journal of Hydrologic Engineering*, 13: 392–399.
- Park S, Oh C, Jeon S *et al.*, 2011. Soil erosion risk in Korean watersheds, assessed using the revised universal soil loss equation. *Journal of Hydrology*, 399: 263–273.
- Pimentel D, Harvey C, Resosudarmo P *et al.*, 1995. Environmental and economic costs of soil erosion and con-

- servation benefits. *Science*, 267: 1117–1123.
- Renard K G, Foster G R, Weesies G A *et al.*, 1991. RUSLE, revised universal soil loss equation. *Journal of Soil and Water Conservation*, 1: 30–33.
- Sharda V N, Mandal D, Ojasvi P R, 2013. Identification of soil erosion risk areas for conservation planning in different states of India. *Journal of Environmental Biology*, 34: 219–226.
- Siakeu J, Oguchi T, 2000. Soil erosion analysis and modelling: A review. *Transactions of the Japanese Geomorphological Union*, 21: 413–429.
- Stroosnijder L, 2005. Measurement of erosion: Is it possible? *Catena*, 2/3: 162–173.
- Sun W Y, Shao Q Q, Liu J Y, 2013. Soil erosion and its response to the changes of precipitation and vegetation cover on the Loess Plateau. *Journal of Geographical Sciences*, 23: 1091–1106.
- Sun W Y, Shao Q Q, Liu J Y *et al.*, 2014. Assessing the effects of land use and topography on soil erosion on the Loess Plateau in China. *Catena*, 121: 151–163.
- Thompson J A, Charles B, Butler A, 2001. Digital elevation model resolution: effects on terrain at tribute calculation and quantitative soil–landscape modeling. *Geoderma*, 100: 67–89.
- Tian Y, Zhou Y, Wu B *et al.*, 2009. Risk assessment of water soil erosion in upper basin of Miyun Reservoir, Beijing, China. *Environmental Geology*, 4: 937–942.
- Valente R O A, Vettorazzi C A, 2008. Definition of priority area for forest conservation through the ordered weighted averaging method. *Forest Ecological Management*, 256: 1408–1417.
- Vrieling A, 2006. Satellite remote sensing for water erosion assessment: A review. *Catena*, 65: 2–18.
- Vrieling A, de Jong S M, Sterk G *et al.*, 2008. Timing of erosion and satellite data: A multi-resolution approach to soil erosion risk mapping. *International Journal of Applied Earth Observation and Geoinformation*, 3: 267–281.
- Wang F, Wang C, 2009. Research for the influences of DEM resolution on topographical factors: A case study of Mengyin County. *Research of Soil and Water Conservation*, 16: 225–230. (in Chinese)
- Wang L H, Huang J L, Du Y *et al.*, 2013. Dynamic assessment of soil erosion risk using landsat TM and HJ satellite data in Danjiangkou Reservoir area, China. *Remote Sensing*, 5: 3826–3848.
- Wischmeier W H, Smith D D, 1965. Predicting Rainfall Erosion Losses from Cropland East of the Rocky Mountains, Handbook No.282. US Department of Agriculture (USDA): Washington, DC, USA.
- Yang Q Y, Yuan B Y, 1991. Natural Environment of Loess Plateau and Its Evolution. Beijing, China: Science Press. (in Chinese)
- Yang S T, Zhu Q, 2000. Effect of man-computer interactive interpretation method in soil erosion survey of large scale by remote sensing. *Journal of Soil and Water Conservation*, 14: 88–91. (in Chinese)
- Zhang S G, Li Y P, Cheng Y D, 2002. Soil erosion and its improvement in Huangjiang Reservoir area in Guangdong province. *Journal of Sediment Research*, 5: 76–80. (in Chinese)
- Zhang X W, Wu B F, Li X S *et al.*, 2012. Soil erosion risk and its spatial pattern in upstream area of Guanting Reservoir. *Environmental Earth Sciences*, 65: 221–229.
- Zhang X W, Wu B F, Ling F *et al.*, 2010. Identification of priority areas for controlling soil erosion. *Catena*, 83: 76–86.
- Zhao X L, Zhang Z X, Liu B *et al.*, 2002. Method of monitoring soil erosion dynamic based on remote sensing and GIS. *Bulletin of Soil and Water Conservation*, 22: 29–32. (in Chinese)
- Zhou W F, Wu B F, 2005. Overview of remote sensing approaches to soil erosion monitoring. *Remote Sensing Technology and Application*, 20 (5): 537–542. (in Chinese)
- Zhou W F, Wu B F, Li Q Z, 2005. Spatial and temporary change analysis of soil erosion intensity in recent 20 years in the upper basin of Guanting reservoir. *Research of Soil and Water Conservation*, 12: 183–186. (in Chinese)
- Zhou X, Yang S T, Liu X Y *et al.*, 2015. Comprehensive analysis of changes to catchment slope properties in the high-sediment region of the Loess Plateau, 1978–2010. *Journal of Geographical Sciences*, 25: 437–450.
- Zhu M Y, 2012. Soil erosion risk assessment with CORINE model: Case study in the Danjiangkou Reservoir region, China. *Stochastic Environmental Research and Risk Assessment*, 26: 813–822.